Market-Based Congestion Management in Electric Power Systems with Increased Share of Natural Gas Dependent Power Plants

Miloš Pantoš

University of Ljubljana, Faculty of Electrical Engineering, Tržaška 25, SI-1000, Ljubljana, Slovenia
E-mail: milos.pantos@fe.uni-lj.si, Tel.: +386 1 4768241, Fax: +386 1 4264651

Abstract

The paper addresses market-based congestion management (MBCM) in electric power systems taking into account the constraints of the electric power system (EPS) and the natural gas system (NGS). The proposed method is based on the countertrade methodology, where the system operator performs minimum-cost redispatching according to bids from generators and loads. The EPS is presented by the DC model for power flow calculation, which uses power transfer distribution factors (PTDFs) to describe the relation between generators/loads and line-power flows. The proposed solution applies the Benders decomposition method to decouple the problem into a master problem and subproblem. The master problem includes the bid-based redispatching for congestion relief and the EPS feasibility check. The subproblem checks the NGS operation feasibility when gas-fired generating units are redispatched in the master problem. Any NGS violations from the subproblem are incorporated into the master problem as power constraints for the next iteration of congestion management. The master problem is solved by linear programming. The NGS is presented in a nonlinear model and its feasibility check is performed using successive linear programming. Case studies illustrate the applicability of the proposed congestion management method on simple test models of the EPS and the NGS.

Keywords

Benders decomposition, electric power system, linear programming, market-based congestion management, natural gas system, optimization.

1 Nomenclature

Indices:

a, b	Subscript indices of EPS buses
i, j	Subscript indices of NGS buses
k	Subscript index of bidding participant
(k)	Superscript index of k-th iteration
$(k+1)$	Superscript index of k-th iteration
min, max	Superscript indices for minimum and maximum value
p	Subscript index of generator/load bid for MBCM
^	Superscript index of current iteration

Variables and functions:

$A_{(\cdot)(\cdot)}$	Element of node – gas provider incidence matrix
$B_{(\cdot)(\cdot)}$	Element of node – gas load incidence matrix
$c_{(\cdot),(\cdot)}$	Bid price of participant in MBCM
$f_{(\cdot)(\cdot)}$	Natural gas flow on path
$F_{(\cdot)(\cdot)}$	Natural gas consumption of compressor
$g_{(\cdot)}$	Nodal natural gas mismatch
$G_{(\cdot)(\cdot)}$	Element of gas withdrawing node – compressor incidence matrix

$H_{(\cdot)(\cdot)}$	Power of compressor
$L_{(\cdot)}$	Nodal natural gas load
$P_{(\cdot)(\cdot)}$	Active power flow on path
$P_{(\cdot)}$	Injected active power of generator/load
$PTDF_{(\cdot)(\cdot),(\cdot)}$	PTDF of generator/load on path
$Q_{(\cdot)(\cdot)}$	Reactive power flow on path
$Q_{(\cdot)(\cdot),0}$	Initial reactive power flow on path
$Q_{(\cdot)}$	Injected nodal reactive power of generator/load
$R_{(\cdot),(\cdot)}$	Pressure ratio of compressor
$s_{(\cdot)}$	Total cost of participant in MBCM
$s_{(\cdot),(\cdot)}$	Cost of active power change bid from participant in MBCM
$S_{(\cdot)(\cdot)}$	Apparent power flow on path
$SL_{(\cdot)}$	Nodal slack variable
$v_{(\cdot)}$	Nodal natural gas supply
$\Delta P_{(\cdot)(\cdot)}$	Change of active power flow on path
$\Delta P_{(\cdot)}$	Total active power change of participant in MBCM
$\Delta P_{(\cdot),(\cdot)}$	Active power change bid from participant in MBCM
ω	Objective function of NGS subproblem
$\pi_{(\cdot)}$	Nodal gas pressure

Parameters and constants:

$a_{(\cdot)(\cdot)}$, $b_{(\cdot)(\cdot)}$, $\alpha_{(\cdot)(\cdot)}$	Parameters of compressor
$C_{(\cdot)(\cdot)}$	Parameter of pipeline
$GC_{(\cdot)}$	Set of gas nodes connected to node
$k_{(\cdot)(\cdot)}$, $d_{(\cdot)(\cdot)}$, $e_{(\cdot)(\cdot)}$	Gas consuming parameters of compressor
M	Large numerical constant
$n_{(\cdot)}$	Number of bids of participant in MBCM
NC	Number of compressors
NGL	Number of natural gas loads
NGS	Number of natural gas suppliers
NN	Number of nodes in NGS
NP	Set of all bidding participants in MBCM
$p_{(\cdot)}$, $q_{(\cdot)}$, $r_{(\cdot)}$	Gas consumption coefficients of gas-fired units
ε	Infinitesimal numerical constants

Matrices and vectors:

A	Node – gas provider incidence matrix
B	Node – gas load incidence matrix
D	Gas node – branch incidence matrix
f	Matrix of natural gas flows
F	Matrix of gas consumption of compressors
g	Matrix of natural gas mismatches

$\mathbf{G}$	Gas withdrawing node – compressor incidence matrix
$\mathbf{H}$	Matrix of compressor powers
$\mathbf{J}$	Jacobian matrix for NGS
$\mathbf{J}_{\pi}$, $\mathbf{J}_{H}$	Jacobian submatrices for NGS
$\mathbf{L}$	Matrix of gas loads
$\mathbf{P}$	Matrix of active power injections
$\mathbf{SL}$	Matrix of slack variables
$\mathbf{v}$	Matrix of natural gas supplies
$\mathbf{x}$	Vector of unknown variables
$\boldsymbol{\mu}$	Vector of dual variables in NGS subproblem
$\boldsymbol{\pi}$	Matrix of nodal natural gas pressures

Abbreviations:

EPS	Electric power system
FOR	Forced outage rate
LOEP	Loss of energy probability
LP	Linear programming
MBCM	Market-based congestion management
NGS	Natural gas system
PTDF	Power transfer distribution factor
TSO	Transmission system operator

2 INTRODUCTION

The process of unbundling has provided open access to transmission networks and resulted in a large number of new players having entered the electricity market, where generation companies offering cheaper power are the preferred suppliers to loads. Transmission lines may operate at or beyond their limits, thereby causing network congestions. Due to the resulting network constraints, it is not possible to accommodate all desired transactions. Congestion management is an ancillary service in a deregulated environment and the responsibility of system operators. Nowadays we are witnessing a lack of new investments into transmission paths or their slower realization, although the needs are growing as a result of load increase. In order to provide system security, stability and, indirectly, ensure a reasonable cost of electric energy, system operators need effective tools to prevent transmission paths from overloading and to allow market players to maximize the use of the network.

Among several various congestion management approaches [1]–[5], two well-known approaches to congestion management in a deregulated environment stand out in particular, i.e. the zonal pricing approach and the countertrade approach. Under the zonal pricing approach the power systems are split into different zones connected by frequently congested lines. In case of congestion, a different market clearing price is set in each zone in such a manner that trading between zones results in power flows that are smaller or equal to the transfer capability. If there is no congestion between the zones, their market clearing price is uniform. The problem with zonal pricing is that it does not prevent internal congestion, since the zonal boundaries are defined ex-ante. To account for this deficiency, the countertrade approach is often utilized.

With the countertrade approach the system operator redispatches power in such a way that the resulting power flows do not overload any lines. Market players can bid to increase or decrease their production and/or consumption in a similar manner as this is done in a balancing market, while the responsibility of the system operator is to select bids in the most efficient way. The countertrade congestion management approach utilizing Generalized Generation Distribution Factors (GGDFs) [6] to obtain the relation between redispatched power and change of line power flow was presented in [7]. Due to the nature of these factors, LP was used to obtain an optimal redispatch of power production. In case of load redispatch, loads are considered as negative injections and GGDFs are calculated in the same manner as for generators, which enables a simultaneous redispatch of generators and loads.

Aside from energy deficit and rising electricity prices today we are also witnessing increasing interdependency of EPSs and NGSs, which is due to the rising number of natural gas dependent power plants, such as gas-fired and combined-cycle power plants. They have several major attributes as compared to conventional coal plants, including high efficiency, lower cost of capital investment, lower environmental impact, expeditious permitting and operation flexibility. Through natural gas-fired production units NGSs affect the security and the economics of EPSs. Security issues include pressure losses, pipeline contingencies and lack of storage or natural gas supply disruptions, which may lead to forced outages of multiple gas-fired units or deration of generating capacity. This can dramatically increase operating costs and congestion, and thus jeopardize the security of EPSs. A solution to the problem of congestion management is therefore needed and it should be based on the integration and simultaneous analysis of EPS and NGS models, as discussed in this paper.

Literature proposes several models of integration of EPSs and NGSs, addressing different problems in the field of power system operation and planning. The two-phase nonlinear optimization model is proposed in [8], which models the integrated operation of NGSs and EPSs. A nonlinear optimization model is proposed in [9] and [10], which merges the traditional optimal power flow and natural gas transmission constraints. The short-term scheduling of integrated natural gas transmission and hydrothermal power systems is considered in [11], which applies the Lagrangian relaxation and dynamic programming. The impact of natural gas transmission charges on power markets is discussed in [12]. Long-term integrated planning is analyzed in [13], showing that decisions in natural gas and power transmission systems are highly interdependent. The piecewise linear approximation of nonlinear flow-pressure relations is modeled in the UC problem in [14]. The security-constrained unit commitment with natural gas transmission constraints is addressed in [15], where NGS is presented by a nonlinear model and iteratively solved by the Newton–Raphson method.

The research presented in this paper was motivated by the following facts:

- overloading of transmission lines due to increasing demand/production, and lack of new investments into transmission lines,
- higher interdependency and interoperability of EPSs and NGSs due to an increasing share of natural gas-fired generating units,
- required effective market-based solution for congestion management.

The paper thus proposes a new MBCM method with EPS and NGS constraints. The main idea derives from [7] but is upgraded, as GGDFs are replaced by Power Transfer Distribution Factors (PTDFs), which present the impact of generators/loads on active power flows and also allow for simultaneous bidding of generators and loads in the proposed MBCM. The actual advantage of these factors is their wide utilization in numerous applications in advanced power system operation and maintenance, planning, and market monitoring. Compared to [7] the novelty of the proposed MBCM is the feasibility check of the NGS operation. The proposed MBCM uses successive LP to apply a nonlinear model of the NGS. It is presented in detail in [15].

The optimization problem is decomposed into the master problem dealing with optimal redispatching and the EPS feasibility check, and the subproblem addressing the NGS feasibility check, if gas-fired generating units are redispatched in the master problem. Any violations in the subproblem are incorporated into the master problem through the Benders loop as power constraints for the next iteration of congestion management.

The main contribution of the proposed approach is inclusion of NGS constraints into MBCM derived from [7]. This improvement requires implementation of iterative methods for NGS feasibility check and Benders decomposition.

The rest of this paper is organized as follows: Generation and load redispatch are presented in Section 3. Modeling of NGSs is presented in Section 4. The MBCM model integrating NGS constraints is formulated in Section 5. Section 6 presents and discusses in detail a six-bus EPS with a two-node NGS and the IEEE 39-bus system with a 12-node NGS. The conclusion drawn from the study is provided in Section 7.

3 Generation and Load Redispatching

In the market environment, generators and loads trade in electric energy. As a result, for each moment initial values of injected nodal powers are known, which determine power flows through the system according to its topology. In case of congestions on the transmission lines, the system operator is responsible for power redispatching in order to eliminate overloading.

In the proposed market-based approach generators and loads provide their adjustment bids for active power increases and/or decreases at a specific price for a certain moment when congestions occur. Figure 1 presents the bidding curve of participant k with n_k sections, i.e. bids. If generators are considered, the left-hand side of the curve presents the cost function of power reduction and the right-hand side the cost function of power increase. Since loads are interpreted as negative injections, the left-hand side of the curve in Figure 1 presents the cost function of load increase and the right-hand side the cost of load decrease. The cost of the p-th bid for power change of participant k, $\Delta P_{k,p}$, is $s_{k,p}(\Delta P_{k,p})$ and the bid price, $c_{k,p}$, can be calculated as:

$$c_{k,p} = \frac{s_{k,p}\left(\Delta P_{k,p}\right)}{\Delta P_{k,p}} . \tag{1}$$

The system operator has to sort increase and decrease offers in ascending order according to price, so as to utilize the cheapest offers first and therefore achieve an optimal redispatch of production and load. The objective function is:

$$Min\left\{ \sum_{k \in NP} s_k \right\} , \tag{2}$$

where NP is the set of all bidding participants. The total cost of participant k in (2) is expressed as:

$$s_k = \sum_{p=1}^{n_k} s_{k,p}\left(\Delta P_{k,p}\right). \tag{3}$$

The minimum costs of redispatching have to be achieved taking into account several technical constraints of the EPS:

- operation limits of generators and loads:

$$P_k^{\min} \le P_k + \Delta P_k \le P_k^{\max} , \tag{4}$$

- active power balance in the EPS:

$$\sum_{k \in NP} \Delta P_k = 0 , \tag{5}$$

- limits of transmission paths:

$$P_{ab}^{\min} \le P_{ab} + \Delta P_{ab} \le P_{ab}^{\max} . \tag{6}$$

P_k and ΔP_k in (4) and (5) present the injected active power of generator/load k in MBCM and its total active power change, which is expressed as:

$$\Delta P_k = \sum_{p=1}^{n_k} \Delta P_{k,p} . \tag{7}$$

In (6), P_{ab} presents the active power flow on path a–b. In order to express the active power flow change on path a–b, ΔP_{ab}, in (6) with the optimization variable $\Delta P_{k,p}$, PTDFs are introduced as:

$$PTDF_{ab,k} = \frac{\Delta P_{ab}}{\Delta P_k} , \tag{8}$$

and present the impacts of generators/loads, ΔP_k, on the active power flows on the path a–b, ΔP_{ab}. Consequently, ΔP_{ab} in (6) is expressed as:

$$\Delta P_{ab} = \sum_{k \in NP} \left(\Delta P_k \cdot PTDF_{ab,k} \right). \tag{9}$$

To calculate the change of active power flow on path a–b, ΔP_{ab}, in (9), the PTDF of generator/load k on path a–b, $PTDF_{ab,k}$, is multiplied by the power changes of accepted bids of generator/load k by the system operator, ΔP_k. In (5), the transmission losses are neglected due to the DC model of the EPS being applied.

Maximum line currents are usually defined in such a way so as to result in maximum allowed apparent power flows. As only active power flows are considered due to utilization of DC power flows, the proposed method only uses active power limits. It is presumed that the reactive power flows remain unchanged with the redispatch of active power production/load, thus the upper limit of active power flow on path a–b is expressed as:

$$P_{ab}^{\max} = \sqrt{\left(S_{ab}^{\max}\right)^2 - \left(Q_{ab,0}\right)^2} \ , \tag{10}$$

where $S_{ab}^{\max}$ and $Q_{ab,0}$ present the maximum apparent power flow and the reactive power flow on path *a–b* in the initial operating state. This assumption introduces a certain error that can be neglectable, if reactive power flows does not change significantly due to operation of EPS or are relatively small comparing to the active power flows. The assessment of these errors is performed in Section 6. The lower limit of active power flow is defined as:

$$P_{ab}^{\min} = -P_{ab}^{\max} \ , \tag{11}$$

which enables fully exploitation of transmission paths in both directions.

4 Modeling of Natural Gas Transmission System

NGSs are designed to carry natural gas from gas fields to customers. Similar to EPSs, NGSs are very complex nonlinear systems with dynamic behavior. For the purpose of the proposed MBCM in this paper, a steady-state model of the NGS is applied, as presented in [15].

4.1 Elements of NGSs

Usually, NGSs are comprised of natural gas wells, high-pressure and low-pressure transmission pipelines, compressors, storage facilities and residential, commercial and industrial natural gas consumers. Gas-fired power plants represent the most important industrial gas loads, which link EPSs and NGSs. The elements of NGSs are connected through nodes with associated gas pressures. Natural gas suppliers and consumers are modeled as positive and negative natural gas injections in nodes, respectively, while pipelines and compressors present branches with associated natural gas flows.

In the paper, each natural gas supplier is modeled as a positive gas injection limited by maximum and minimum capacity, in case of node *i*:

$$v_i^{\min} \le v_i \le v_i^{\max} \ . \tag{12}$$

Gas loads are represented as negative gas injections limited by upper and lower limits, in case of node *i*:

$$L_i^{\min} \le L_i \le L_i^{\max} \ . \tag{13}$$

Gas storages are categorized based on their capacity and operating parameters. However, for the MBCM of EPSs, they are either modeled as loads or suppliers, thus their capacities are limited as in (12) and (13). The exceptions are self-owned storage facilities of gas-fired power plants, as discussed later in the paper.

Natural gas flows through pipelines depend on nodal pressures and technical parameters, such as the length and the diameter of pipelines, operating temperatures and pressures, types of natural gas, altitude change over the transmission path and the roughness of pipelines. This paper applies the model used to design or optimize natural gas pipeline systems, as presented in [16]–[19]. The gas flow in the pipeline extending from gas node *i* to gas node *j* is modeled as:

$$f_{ij} = \mathrm{sgn}(\pi_i, \pi_j) \cdot C_{ij} \sqrt{\left|\pi_i^2 - \pi_j^2\right|} \ , \tag{14}$$

$$\mathrm{sgn}(\pi_i, \pi_j) = \begin{cases} 1 & \pi_i \ge \pi_j \\ -1 & \pi_i < \pi_j \end{cases} , \tag{15}$$

where C_{ij} is the pipeline *i-j* constant that depends on temperature, length, diameter, friction and gas composition.

In order to compensate for the pressure loss caused by pipeline resistance during the transport of natural gas, compressor stations are installed along pipelines. The natural gas flow through the centrifugal compressor *i-j* is modeled as:

$$f_{ij} = \mathrm{sgn}(\pi_i, \pi_j) \frac{H_{ij}}{a_{ij} - b_{ij}\left[\dfrac{\max(\pi_i, \pi_j)}{\min(\pi_i, \pi_j)}\right]^{\alpha_{ij}}}, \tag{16}$$

where a_{ij}, b_{ij} and α_{ij} are empirically obtained parameters corresponding to the compressor *i-j* design [10], [20], [21]. H_{ij} represents the power of compressor *i-j* as a control variable, where maximum and minimum values have to be considered:

$$H_{ij}^{\min} \le H_{ij} \le H_{ij}^{\max}. \tag{17}$$

The pressure ratio in (16) is restricted within a feasible range in (18), which is based on compressor characteristics:

$$R_{ij}^{\min} \le \frac{\max(\pi_i, \pi_j)}{\min(\pi_i, \pi_j)} \le R_{ij}^{\max}. \tag{18}$$

Compressor *i-j* would consume additional natural gas, F_{ij}, that can be withdrawn from either inlet node *i* or outlet node *j* of the compressor to drive turbines, as illustrated in Figure 2. F_{ij} represents transmission losses of the natural gas grid and is related to the power of compressor *i-j*, H_{ij}, being calculated as:

$$F_{ij} = k_{ij} + d_{ij} \cdot H_{ij} + e_{ij} \cdot H_{ij}^2, \tag{19}$$

where k_{ij}, d_{ij} and e_{ij} are the natural gas consuming parameters of compressor *i-j*.

4.2 Formulation of natural gas flow conservation equation

In a steady-state condition, the gas flow balance at each node has to be obtained. From the mathematical point of view, the natural gas flow mismatch is equal to zero:

$$\mathbf{g}(\mathbf{v}, \boldsymbol{\pi}, \mathbf{H}, \mathbf{L}) = \mathbf{A} \cdot \mathbf{v} - \mathbf{B} \cdot \mathbf{L} - \mathbf{D} \cdot \mathbf{f} - \mathbf{G} \cdot \mathbf{F} = \mathbf{0} \tag{20}$$

or for node *i*:

$$g_i(\mathbf{v}, \boldsymbol{\pi}, \mathbf{H}, \mathbf{L}) = \sum_{j=1}^{NGS} A_{ij} \cdot v_j - \sum_{j=1}^{NGL} B_{ij} \cdot L_j - \sum_{j \in GC_i} f_{ij} - \sum_{j=1}^{NC} G_{ij} \cdot F_{ij} = 0. \tag{21}$$

By incorporating (14), (16) and (19) into (21), a group of nonlinear equations of the *NN* dimension is obtained, where $NN + NC + NGS + NGL$ are variables involving node pressure, power of each compressor, natural gas supply and natural gas load.

4.3 Interdependency of EPS and NGS

Electric power generated by a gas-fired production unit is a nonlinear function of natural gas supply, presented as a natural gas load in the NGS. The NGS has to supply generator *j* with L_j of natural gas to support its electric power production P_j:

$$L_j = p_j + q_j \cdot P_j + r_j \cdot P_j^2. \tag{22}$$

where coefficients p_j, q_j and r_j depend on the power plant characteristics.

Each gas-fired production unit has its maximum and minimum technical boundary, (4). However, its electric energy production also depends on the natural gas contracts it has entered into with natural gas suppliers, which can impose additional limitations to its production capacity. For simplicity's sake, the gas contract constraints are not explicitly addressed in this paper, since it is presumed that $P_k^{\min}$ and $P_k^{\max}$ in (4) already incorporate possible additional limitations imposed by a natural gas contract.

As previously mentioned, gas storage facilities are modeled as gas loads or suppliers with capacity limitations, (12), (13). The gas-fired units with self-owned storage facilities do not directly affect NGSs, since self-owned storage facilities can be interpreted as energy buffers. Parameters in (22) should therefore be appropriately adjusted for such production units. In this way, self-owned storage facilities are not explicitly modeled as regular storage facilities, but their characteristics are indirectly incorporated into the gas consumption curves, (22).

Gas-fired production units also participate in MBCM, meaning that they also place their bids to the system operator. Each bid comprises offer amount, $\Delta P_{k,p}$, offer price, $c_{k,p}$, and time stamp. References [15], [19], [22] deal with security-constrained unit commitment with NGS constraints and discuss natural gas contract types and natural gas prices. Generally speaking, natural gas prices are directly reflected in the generation costs of gas-fired units, therefore this correlation has to be considered in the MBCM bidding process. In this paper, it is presumed that according to the applied bidding strategy the offers for redispatching already incorporate the influence of all expected costs, including the costs of natural gas supply that would occur due to redispatching. The model therefore only applies the prices for MBCM, $c_{k,p}$.

5 MBCM MODEL WITH INTEGRATED NGS CONSTRAINTS

Figure 3 depicts the MBCM flowchart with NGS constraints. Benders decomposition [23], [24] is applied to decompose the original large-scale optimization problem into the master congestion management (CM) problem and the NGS subproblem, based on the LP duality theory. The system operator executes the bid-based MBCM in the event of transmission congestions. Generators and loads that participate in the bidding process are redispatched in order to satisfy power transmission constraints. If there is no feasible solution, market participants are asked to adjust their offers, followed by the next iteration of MBCM. If a solution is not found, the system operator has to stop bidding and perform technical redispatching, in order to provide a reliable operation of the EPS by eliminating congestions. Meanwhile, the natural gas transmission operator provides the system operator with the information on natural gas loads, suppliers and storage facilities, natural gas network topology and transmission parameters. Next the system operator checks the feasibility of the NGS that supplies natural gas to gas-fired production units by examining the adequacy of natural gas resource capacities for gas production and the capacities of pipelines and compressors for gas transmission. If the natural gas check subproblem proves infeasible, Benders cuts are used to form natural gas usage constraints for gas-fired power plants, and the subproblem is added to the master problem. The iterative process between the master MBCM problem and the natural gas transmission feasibility check subproblem continues until the feasibilities of EPS and NGS are obtained.

5.1 Master MBCM problem

The master MBCM problem is fully defined as:

$$Min\left\{\sum_{k\in NP}\sum_{p=1}^{n_k} s_{k,p}\left(\Delta P_{k,p}\right)\right\}, \tag{23}$$

s.t.

$$P_k^{\min} \le P_k + \sum_{p=1}^{n_k}\Delta P_{k,p} \le P_k^{\max}, \tag{24}$$

$$\sum_{k\in NP}\sum_{p=1}^{n_k}\Delta P_{k,p} = 0, \tag{25}$$

$$-P_{ab}^{\max} \le P_{ab} + \sum_{k\in NP}\left(\left(\sum_{p=1}^{n_k}\Delta P_{k,p}\right)\cdot PTDF_{ab,k}\right) + \le P_{ab}^{\max}. \tag{26}$$

where (23) is the objective function (2) with incorporated (3). It should be pointed out that the social welfare that is commonly used in evaluation of the market design is indirectly incorporated in the objective function. The cost minimization in (23) leads to lower transmission prices since these costs have to be covered by a transmission system operator (TSO) and charged to consumers.

From the market aspect, the impact of proposed MBCM approach on the social welfare can be explained by the demand and supply curves in Figure 4.

If path a–b is congested, ΔP_{ab} on that path is required in order to relive that congestion. Thus ΔP_{ab} presents a completely price inelastic demand of TSO that has to perform redispatching. On the other hand, several bids from generators and loads are provided shaping the supply curve in Figure 4. Each bid consists of the price, $c_{(\cdot),(\cdot)}$, and the power change, $\Delta P_{(\cdot),(\cdot)}$, as presented in Figure 1. Besides lower bid prices, for TSO it is also important to identify those bids that have a significant impact on the power flow on the congested paths, e.g. path a–b. Thus $\Delta P_{(\cdot),(\cdot)}$ on the x axis in Figure 4 has to be multiplied by its impact on the line power flow, i.e. $PTDF_{ab,(\cdot)}$. After the market clearing is performed and the optimal solution is found, the gray area in the Figure 4 presents the social welfare. This area is maximized when the cost minimization proposed in (23) is performed. Redispatched generators and loads are paid as they bided and TSO obtains the lowest prices for the congestion relief on path a-b finally leading to the lower transmission prices for consumers.

Eq. (24) presents the limitation of generators and loads (4) with incorporated (7). Eq. (25) is the active power balance (5) with incorporated (7), while (26) is the transmission line limitation (6) with incorporated (7), (9) and (11). The optimization variables are generator/load shifts, $\Delta P_{k,p}$. The total generator/load shifts are calculated by (7) and the resulting powers of gas-fired production units could be additionally constrained by the NGS feasibility constraints, which is checked in the subproblem.

5.2 NGS feasibility check subproblem

In the natural gas flow balance in (21), the number of variables exceeds the number of equations, and the solution would require fixing no more than $NC + NGS + NGL$ variables with iterative nonlinear optimization techniques. The Newton–Raphson method is applied to solve the nonlinear equations. If **x** represents the vector of unknown variables in (21):

$$\mathbf{x} = \left\{\mathbf{v}, \boldsymbol{\pi}, \mathbf{H}, \mathbf{L}\right\}, \tag{27}$$

the iterative matrix equation is given as:

$$\mathbf{x}^{(k+1)} = \mathbf{x}^{(k)} + \Delta\mathbf{x}^{(k)} = \mathbf{x}^{(k)} - \frac{\mathbf{g}\left(\mathbf{x}^{(k)}\right)}{\mathbf{J}^{(k)}}, \tag{28}$$

where $\mathbf{J}^{(k)}$ is the Jacobian matrix in iteration (k) and is expressed as:

$$\mathbf{J}^{(k)} = \frac{\partial \mathbf{g}\left(\mathbf{x}^{(k)}\right)}{\partial \mathbf{x}}. \tag{29}$$

The nonzero elements of the Jacobian matrix are given as:

$$\frac{\partial g_i}{\partial v_j} = A_{ij}, \tag{30}$$

$$\frac{\partial g_i}{\partial L_j} = -B_{ij}, \tag{31}$$

$$\left.\frac{\partial g_i}{\partial \pi_i}\right|_{\text{pipeline}} = -\sum_{j \in GC(i)} \frac{\partial f_{ij}}{\partial \pi_i} = -\sum_{j \in GC(i)} \begin{cases} M, & \left|\pi_i^2 - \pi_j^2\right| < \varepsilon \\ \dfrac{C_{ij}\pi_i}{\sqrt{\left|\pi_i^2 - \pi_j^2\right|}}, & \left|\pi_i^2 - \pi_j^2\right| \geq \varepsilon \end{cases}, \tag{32}$$

$$\left.\frac{\partial g_i}{\partial \pi_j}\right|_{\text{pipeline}} = -\frac{\partial f_{ij}}{\partial \pi_j} = -1 \cdot \begin{cases} -M, & \left|\pi_i^2 - \pi_j^2\right| < \varepsilon \\ -\dfrac{C_{ij}\pi_j}{\sqrt{\left|\pi_i^2 - \pi_j^2\right|}}, & \left|\pi_i^2 - \pi_j^2\right| \geq \varepsilon \end{cases}, \tag{33}$$

$$\left.\frac{\partial g_i}{\partial \pi_i}\right|_{\text{compressor}} = -\sum_{j\in GC(i)} \frac{\partial f_{ij}}{\partial \pi_i} = -\sum_{j\in GC(i)} \begin{cases} \dfrac{\alpha_{ij} H_{ij} a_{ij} \dfrac{\pi_j^{\alpha_{ij}}}{\pi_i^{\alpha+1}}}{\left[a_{ij}\left(\dfrac{\pi_j}{\pi_i}\right)^{\alpha_{ij}} - b_{ij}\right]^2}, & \pi_i < \pi_j \\ \dfrac{\alpha_{ij} H_{ij} a_{ij} \dfrac{\pi_i^{\alpha_{ij}-1}}{\pi_j^{\alpha_{ij}}}}{\left[a_{ij}\left(\dfrac{\pi_i}{\pi_j}\right)^{\alpha_{ij}} - b_{ij}\right]^2}, & \pi_i \ge \pi_j \end{cases}, \tag{34}$$

$$\left.\frac{\partial g_i}{\partial \pi_j}\right|_{\text{compressor}} = -\frac{\partial f_{ij}}{\partial \pi_j} = -1 \cdot \begin{cases} \dfrac{-\alpha_{ij} H_{ij} a_{ij} \dfrac{\pi_j^{\alpha_{ij}-1}}{\pi_i^{\alpha_{ij}}}}{\left[a_{ij}\left(\dfrac{\pi_j}{\pi_i}\right)^{\alpha_{ij}} - b_{ij}\right]^2}, & \pi_i < \pi_j \\ \dfrac{-\alpha_{ij} H_{ij} a_{ij} \dfrac{\pi_i^{\alpha_{ij}}}{\pi_j^{\alpha_{ij}+1}}}{\left[a_{ij}\left(\dfrac{\pi_i}{\pi_j}\right)^{\alpha_{ij}} - b_{ij}\right]^2}, & \pi_i > \pi_j \end{cases}, \tag{35}$$

$$\frac{\partial g_i}{\partial H_{ij}} = -\sum_{j\in GC(i)} \frac{\partial f_{ij}}{\partial H_{ij}} - \sum_{j=1}^{NC} G_{ij} \cdot (2e_{ij} + d_{ij}), \tag{36}$$

where:

$$\frac{\partial f_{ij}}{\partial H_{ij}} = \begin{cases} \dfrac{1}{a_{ij}\left(\dfrac{\pi_j}{\pi_i}\right)^{\alpha_{ij}} - b_{ij}}, & \pi_i < \pi_j \\ \dfrac{-1}{a_{ij}\left(\dfrac{\pi_i}{\pi_j}\right)^{\alpha_{ij}} - b_{ij}}, & \pi_i > \pi_j \end{cases}, \tag{37}$$

and M and ε are the large and infinitesimal constants that assure numerical stability. A complete derivation of (32)–(37) can be found in [15].

The iterative matrix equation (28) can be reformulated as:

$$\begin{bmatrix} \Delta\boldsymbol{\pi}^{(k)} \\ \Delta\mathbf{H}^{(k)} \\ \Delta\mathbf{v}^{(k)} \\ \Delta\mathbf{L}^{(k)} \end{bmatrix} = -\left(\mathbf{J}^{(k)}\right)^{-1} \mathbf{g}(\boldsymbol{\pi}^{(k)}, \mathbf{H}^{(k)}, \mathbf{v}^{(k)}, \mathbf{L}^{(k)}) \,. \tag{38}$$

Equation (38) incorporates $\mathbf{J}^{(k)}$, which consists of the Jacobian submatrices in iteration (k):

$$\mathbf{J}^{(k)} = \left[\mathbf{J}_{\pi}^{(k)} \quad \mathbf{J}_{H}^{(k)} \quad \mathbf{A} \quad -\mathbf{B}\right]. \tag{39}$$

and the matrix of variable changes between iterative steps (k+1) and (k):

$$\begin{bmatrix} \Delta\boldsymbol{\pi}^{(k)} \\ \Delta\mathbf{H}^{(k)} \\ \Delta\mathbf{v}^{(k)} \\ \Delta\mathbf{L}^{(k)} \end{bmatrix} = \begin{bmatrix} \boldsymbol{\pi}^{(k+1)} \\ \mathbf{H}^{(k+1)} \\ \mathbf{v}^{(k+1)} \\ \mathbf{L}^{(k+1)} \end{bmatrix} - \begin{bmatrix} \boldsymbol{\pi}^{(k)} \\ \mathbf{H}^{(k)} \\ \mathbf{v}^{(k)} \\ \mathbf{L}^{(k)} \end{bmatrix}. \tag{40}$$

The objective of the NGS subproblem is to minimize the sum of slack variables, SL_j, at natural gas nodes:

$$Min\left\{\omega(\hat{\mathbf{L}}) = \sum_{j=1}^{NGL} (SL_j)\right\}. \tag{41}$$

The non-negative natural gas load shedding variables in matrix **SL** are added to ensure that the optimization problem is always feasible. From a physical viewpoint, such slack variables represent virtual natural gas load shedding at each delivery point to eliminate mismatches.

Constraints (42)–(48) represent pressure limits at each node, the maximum/minimum gas delivery mass of each node, the power limit and the pressure ratio range of compressors:

$$\begin{bmatrix} \mathbf{J}_{\pi} & \mathbf{J}_{H} & \mathbf{A} & \mathbf{-B} \end{bmatrix} \begin{bmatrix} \Delta\boldsymbol{\pi} \\ \Delta\mathbf{H} \\ \Delta\mathbf{v} \\ \Delta\mathbf{L} \end{bmatrix} = -\mathbf{g}(\boldsymbol{\pi}, \mathbf{H}, \mathbf{v}, \hat{\mathbf{L}}) \quad \boldsymbol{\mu}\,, \tag{42}$$

$$\mathbf{SL} + \Delta\mathbf{L} = \mathbf{0}\,, \tag{43}$$

$$-\hat{\mathbf{L}} \le \Delta\mathbf{L} \le \mathbf{0}\,, \tag{44}$$

$$\boldsymbol{\pi}_{\min} \le \boldsymbol{\pi} + \Delta\boldsymbol{\pi} \le \boldsymbol{\pi}_{\max}\,, \tag{45}$$

$$\mathbf{v}_{\min} \le \Delta\mathbf{v} + \mathbf{v} \le \mathbf{v}_{\max}\,, \tag{46}$$

$$\mathbf{H}_{\min} \le \mathbf{H} + \Delta\mathbf{H} \le \mathbf{H}_{\max}\,, \tag{47}$$

$$\mathbf{R}_{\min} \cdot \left(\boldsymbol{\pi}_j + \Delta\boldsymbol{\pi}_j\right) \le \boldsymbol{\pi}_i + \Delta\boldsymbol{\pi}_i \le \mathbf{R}_{\max} \cdot \left(\boldsymbol{\pi}_j + \Delta\boldsymbol{\pi}_j\right), \tag{48}$$

Since natural gas flow equations are nonlinear, successive LP is applied, as proposed in [15], to solve the problem iteratively with the following steps:

1. Initialization of optimization variables.
2. Calculation of the modified Jacobian matrix in (39) and the initial natural gas node mismatch vector $-\mathbf{g}(\boldsymbol{\pi}, \mathbf{H}, \mathbf{v}, \hat{\mathbf{L}})$ based on the initial natural gas loading, the system states and the generation schedules of natural gas providers.
3. LP optimization of the objective function (41) and calculation of changes in state and control variables $\Delta\boldsymbol{\pi}$, $\Delta\mathbf{H}$, $\Delta\mathbf{v}$, and $\Delta\mathbf{L}$. If the difference between the current and previous iterative changes is less than the specified threshold ε, the process is stopped. Otherwise, Step 3 is performed.
4. Update of state and control variables, and calculation of the Jacobian matrix and $\mathbf{SL}$.

Once the above iterative process is completed, a non-negative objective function (41) is obtained. If its value is greater that the specified tolerance ε, the available natural gas resources and controllable compressors cannot satisfy natural gas transmission limits and/or natural gas demands of gas-fired units redispatched by the master MBCM problem. Consequently, the Benders cut is formed:

$$\omega(\mathbf{L}) = \omega(\hat{\mathbf{L}}) + \boldsymbol{\mu}^{\mathrm{T}}\mathbf{B}\left(\mathbf{L} - \hat{\mathbf{L}}\right) \le 0\,. \tag{49}$$

Here, $\omega(\hat{\mathbf{L}})$ is equal to the sum of slack variables in the current iteration. A positive $\omega(\hat{\mathbf{L}})$ corresponds to a positive natural gas node mismatch $-\mathbf{g}(\boldsymbol{\pi}, \mathbf{H}, \mathbf{v}, \hat{\mathbf{L}})$. Symbol $\boldsymbol{\mu}$ presents the dual variable corresponding to (42), which captures the sensitivity of $\omega(\hat{\mathbf{L}})$ to the right-hand mismatch $-\mathbf{g}(\boldsymbol{\pi}, \mathbf{H}, \mathbf{v}, \hat{\mathbf{L}})$, which is derived by solving the dual problem of successive LP. $\boldsymbol{\mu}$ can therefore capture the natural gas node mismatch and feed the information back to the master MBCM problem. By incorporating (22) into (49), power constraints (50) are formed and added to the master problem for the next iterative solution of MBCM:

$$\omega(\mathbf{P}) = \omega(\hat{\mathbf{P}}) + \boldsymbol{\mu}^{\mathrm{T}}\mathbf{B}\left(\mathbf{P} - \hat{\mathbf{P}}\right) \le 0\,. \tag{50}$$

Benders cuts (50) are generated from the solution to the successive approximation of a nonlinear equation. Pipeline equations may make the subproblems non-convex in feasible sets. So if the initial operating point of the natural gas problem is not close enough to the global optimal points, the final solution of MBCM with natural gas constraints may result in a local optimal solution. However, different initial points of natural gas flow should be examined to find the best possible solution. Reference [25] introduces a set of initial points, π_i, π_j, to linearize (14), which can replace the nonlinear function with linear inequality for each pipeline. For any given pipeline flow, only one of the inequality constraints, namely the one that approximates the flow best, will be binding. For a pipeline network without compressors, (41)–(48) represent a LP problem rather than successive LP, when applying linearized inequality constraints [25]. The improvement can potentially enhance the quality of the optimal solution with the same computing time. This question is not addressed in the paper.

5.3 Coordinated long-term planning of EPS and NGS

Increased share of natural gas dependent power units require coordinated long-term planning of EPS and NGS. In the addressed problem of congestion relieves, the appropriate planning approach would reduce violations of NGS constraints in the NGS feasibility check subproblem presented in Subsection 5.2 and would enable unconstrained redispatching of gas-fired generating units in the proposed MBCM solution.

As mentioned, [12] and [13] are dealing with coordinated planning of EPSs and NGSs using integrated models of both systems. Beside a tool for a simultaneous analysis of electricity and gas markets, [12] gives an overview of main identified parameters and constraints that should be considered in the planning process. In [13], a natural-gas network model includes a natural-gas well and pipelines whereas the electrical system includes hydrothermal power generation and a transmission system. A mathematical model of this problem is formulated as a multistage optimization problem where the objective function is to minimize the integrated gas-electricity investment and operation costs. In [26] and [27], stochastic planning procedures of electric energy sources and transmission paths in EPS are proposed. The idea is to expand these approaches to the coordinated stochastic planning of EPS and NGS. Since the planning issue is not the main focus of the paper, the idea is briefly presented here and will be assessed in detail in the future work.

Figure 5 proposes the optimization approach, where the planning procedure consists of:

- input data preparation with the long-term electric and natural-gas consumption forecast, and the list of candidate investment projects,
- Monte Carlo Simulation of possible operating states as a part of a stochastic approach,
- optimization procedure applying LP.

For each analyzed year, the forecasted yearly consumption of electric energy and natural-gas is presented by the annual load duration curve as presented in Figure 6. This curve can be simplified and presented by load blocks, each with a constant power.

Monte Carlo method can be used to create scenarios that simulate random characteristics of system components and load growth. For EPS and NGS elements, their forced outage rates (FORs) are defined according to the past observation of their operation. Once the scenarios are prepared, their set can be efficiently reduced applying GAMS/SCENRED tool, [28] and [29], as proposed in [27].

For each scenario, the optimization procedure in Figure 5 is performed. It is decomposed by the Benders method into the master problem and its subproblem. The master problem is dealing with the cost-based selection, i.e. cost minimization of future investments in EPS and NGS such as electric generators, natural gas wells, electric and natural-gas infrastructure etc.. The subproblem is addressing the EPS reliability check and the NGS feasibility check. The reliability check is performed as proposed in [26] and [27], where Loss of energy probability (LOEP) is used as a target criterion. If the reliability criterion is not satisfied, additional constraints, i.e. Benders cuts, are formed and included in the master problem. The feasibility check is presented in Subsection 5.2.

Finally, the long-term planning program is obtained that has to be followed in order to obtain a certain level of reliable operation of EPS and NGS. If it is planned to perform the proposed MBCM also by managing NGS operation, its exploitation has to be foreseen and accounted for in the stage of input data preparation. Redispatched gas-fired production units require additional natural-gas consumption that has to be considered in the forecasts, thus the load curve in Figure 6 has to be modified as presented in Figure 7.

6 CASE STUDIES

The proposed method for MBCM with NGS constraints is tested on a simple six-bus model of the EPS that operates interdependently with a two-node NGS, and the IEEE 39-bus system with a 12-node NGS.

6.1 Six-bus EPS and two-node NGS

The coordinated operation of the EPS and the NGS, and MBCM are presented by analyzing a six-bus EPS and a two-node NGS in Figure 8. In the initial operating state, four generators, each producing 250 MW, supply the load of 1,000 MW at node 6. Generator 3 is a natural gas-fired unit supplied with 3,705 kcf of natural gas from node 2 in the NGS. Gas is transported through pipeline 1–2 with C_{12} = 50 kcf/Psig from gas well 1 with nodal pressure π_1 = 150 Psig. The gas consumption coefficients in (13) of gas-fired unit 3 are p_3 = 180 kcf, q_3 = 14 kcf/MW, r_3 = 0.0004 kcf/MW^2.

Five cases are simulated in order to discuss the impact of certain constraints in the EPS and the NGS on MBCM:

- case A without any constraints, i.e. the initial operating state in Figure 8,
- case B with the transmission capacity of line 5–6 limited to 400 MW,
- case C with the transmission capacity of line 5–6 limited to 400 MW, and the maximum natural gas production of well 1 set at 4,000 kcf,
- case D with the transmission capacity of line 5–6 limited to 400 MW, and the required 120 Psig of minimum load pressure at node 2 causing the 4,500 kcf limitation of the pipeline 1–2 transportation capacity,
- case E with the transmission capacity of line 5–6 limited to 400 MW, and added compressor at the end of pipeline 1–2, with parameters in Tables 1 and 2.

The results for all five cases are presented in Table 3. In the initial state, i.e. case A, the generators produce 250 MW each and MBCM is not performed since transmission lines are not congested. In cases B–E, the generators place bids at the MBCM auction offering the prices of \$10/MW, \$20/MW, \$15/MW and \$30/MW, respectively. In the case of congested line 5–6, generators 1 and 2 compete for power reduction, with generator 1 taking the lead due to its lower bid price. Similarly, generators 3 and 4 compete for power increase, with generator 3 being cheaper but not necessarily in the lead, as it can be constrained by the NGS due to being a gas-fired production unit. In case B, generator 1 decreases and generator 3 increases power to 150 MW and 350 MW, respectively. Consequently, the natural gas supply of generator 3 is increased and the NGS is additionally loaded, resulting in a pressure decrease at gas node 2. The cost of MBCM is equal to \$2,500.

Compared to case B, case C additionally simulates the shortage of gas supply from well 1. The power of generator 3 decreases from 350 MW in case B to 270.76 MW in order to meet the gas production capacity of well 1. Since the NGS is less loaded, the pressure at gas node 2 rises, contrary to the previous case. Due to the power decrease of generator 3, generator 4 with the bid price of \$30/MW is redispatched in order to eliminate the congestion, resulting in higher costs of MBCM.

Pressures in the NGS are analog to voltages in the EPS, thus the pressure limitations for gas nodes should be observed in order to maintain a reliable operation of the NGS and consequently of the EPS. Case D introduces the 120 Psig minimum pressure value at gas node 2. Since pressure 1 is predefined, the pressure difference between node 1 and 2 limits the transportation capacity of pipeline 1–2 to 4,500 kcf. Due to these constraints, the power of generator 3 is reduced from 350 MW in case B to 305.9 MW in order to meet the pressure limit at node bus 2. Since the power of generator 4 increases, the costs of MBCM also rises compared to the costs in case B.

The last case presents the role of natural gas compressors in the NGS. Similar to the transformers in the EPS that regulate voltages, compressors regulate pressures in the NGS. In case E the compressor is added at the end of pipeline 1–2, as presented in Figure 9. The results in Table 3 show that the pressure of gas node 2 is equal to 178.30 Psig, which is above the 120 Psig limit, thus generator 3 is not constrained by the NGS and produces 350

MW. Since generator 4 is not redispatched as in case D, the costs of MBCM in case E are equal to the costs of MBCM in case B. Compared to case D, costs are reduced and the compressor saves \$661.5 due to MBCM.

6.2 IEEE 39-bus system and 12-node NGS

The IEEE 39-bus EPS model in Figure 10 and the 12-node NGS model in Figure 11 are used to study MBCM with natural gas transmission constraints. The IEEE 39-bus system consists of 12 transformers, 34 lines and 10 generators, of which generators 34, 37 and 38 are gas-fired units supplied with natural gas from nodes 12, 5, 11, respectively. 8 loads of the 12-node NGS are supplied by three natural gas wells through 8 pipelines and two compressors. The parameters of the EPS and NGS models used are given in Tables A.1–A.8 in the Appendix.

Three cases are studied and compared in order to present MBCM with NGS constraints:

- case A without any EPS or NGS constraints, i.e. the initial operating state,
- case B with transmission capacities of lines 5–6 and 16–17 decreased to 400 MVA and 170 MVA, respectively, and without any NGS constraints,
- case C with transmission capacities of lines 5–6 and 16–17 decreased to 400 MVA and 170 MVA, respectively, and with NGS constraints.

To make the present paper as clear as possible, only generators are presumed to be bidding in all cases. Loads are considered negative generators and can thus be easily included in the bidding process. Table 4 presents the bids of generators that participate in MBCM.

The results of all simulated cases are presented in Table 5. In case A with no transmission congestion, generation dispatching is not performed and the cost of MBCM equals 0. The initial reactive power flows on lines 5–6 and 16–17 equal 35.48 MVAr and 12.23 MVAr, respectively. These values are used to calculate the active power transmission capacities of the lines, (10).

In case B, only EPS constraints are considered, resulting in a generation redispatch according to the proposed bids; the costs of MBCM are \$4,613.7. It should be pointed out that the apparent power flow on line 16–17 is 10.40 % higher from the allowed maximum flow of 170 MVA, since the reactive power flow of 8.99 MVAr in case B differs considerably, i.e. by 26.49 %, from the initial reactive power flow of 12.23 MVAr. The proposed method presumes that reactive power flows do not change considerably, and uses (10) to transform the apparent power flow limits into active power flow limits used in MBCM. In case of line 5–6, the difference between the reached apparent power flow of 399.67 MVA and the upper limit of 400 MVA is 0.08 %, since the reactive power flow of 30.19 MVAr on this line in case B does not differ considerably, i.e. only by 14.91 %, from the initial reactive power flow of 35.48 MVAr.

Case C considers NGS constraints in MBCM. Due to additional limitations of generators 37 and 38, their power increases are limited to 70.10 MW and 0.15 MW, respectively. Consequently, in order to eliminate congestions on lines 5–6 and 16–17, the power of the more expensive generators 30, 36 is increased. Generators 31, 32 and 34 decrease their power. As a result of generation redispatching with additional NGS constraints, the costs of MBCM here are \$5,922 and thus higher than in case B.

7 CONCLUSIONS

This paper proposes a new method of MBCM with natural gas transmission constraints. To avoid the computational complexity of solving the proposed large-scale optimization problem, Benders decomposition is applied to separate the master MBCM problem and the natural gas transmission subproblem. In the countertrade MBCM model, a bid-based generation/load redispatching is performed, utilizing PTDFs in order to obtain the relation between redispatched power and change of power flows. Successive LP is applied in the natural gas transmission feasibility check. The idea of the proposed MBCM approach with natural gas transmission constraints is presented in the case study of the interdependent operation of a six-bus model of the EPS and a two-node model of the NGS. The effectiveness of the proposed solution is demonstrated on the case of the interdependent operation of an IEEE 39-bus system and a 12-node NGS.

APPENDIX A

Tables A.1–A.8 present parameters of an IEEE 39-bus EPS and a 12-node NGS that operate interdependently.

8 REFERENCES

[1] Androcec I, Wangensteen I. Different Methods for Congestion Management and Risk Management. Proceedings 9th International Conference on Probabilistic Methods Applied to Power Systems 2006; 1-6.

[2] Glavitsch H, Alvarado F. Management of multiple congested conditions in unbundled operation of a power system. IEEE Transactions on Power Systems 1998; 3(3): 1013-1019.

[3] Chanana S. Kumar A. Power Flow Contribution Factors based Congestion Management with Real and Reactive Power Bids in Competitive Electricity Markets. Proceedings of 2007 IEEE/PES General Meeting 2007; 1-8.

[4] Krause T, Andersson G. Evaluating Congestion Management Schemes in Liberalized Electricity Markets Using an Agent-based Simulator. Proceedings of 2006 IEEE/PES General Meeting 2006; 8.

[5] Song H, Kezunovic M. A Comprehensive Contribution Factor Method for Congestion Management. Proceedings of 2004 Power Systems Conference and Exposition 2004; 977-981.

[6] Ng WY. Generalized Generation Distribution Factors for Power System Security Evaluations. IEEE Transactions on Power Apparatus and Systems 1981; PAS-100(3): 1001-1005.

[7] Grgič D, Gubina F. Congestion Management Approach after Deregulation of the Slovenian Power System. Proceedings of 2002 Power Engineering Society Summer Meeting 2002; 3: 1661-1665.

[8] Munoz J, Jimenez-Redondo N., Perez-Ruiz J, Barquin J. Natural gas network modeling for power systems reliability studies. Proceedings of 2003 Power Tech Conference 2003; 4: 8.

[9] Unsihuay C, Marangon Lima JW, Zambroni de Souza AC. Modeling the Integrated Natural Gas and Electricity Optimal Power Flow. Proceedings of 2007 IEEE/PES General Meeting 2007; 1-7.

[10] An S, Li Q, Gedra TW. Natural gas and electricity optimal power flow. Proceedings of 2003 IEEE/PES Transmission and Distribution Conference and Exposition 2003; 1: 138-143.

[11] Unsihuay C, Marangon Lima JW, Zambroni de Souza AC. Short-term operation planning of integrated hydrothermal and natural gas systems. Proceedings of 2007 IEEE/PES Power Tech Conference 2007; 1410-1416.

[12] Morals MS, Marangon Lima JWM. Natural Gas Network Pricing and Its Influence on Electricity and Gas Markets. Proceedings of 2003 IEEE Bologna Power Tech Conference 2003; 3: 6.

[13] Hecq S, Bouffioulx Y, Doulliez P, Saintes P. The Integrated Planning of the Natural Gas and Electricity Systems under Market Conditions. Proceedings of 2001 IEEE Porto Power Tech Conference 2001; 1: 5.

[14] Urbina M, Li Z. A Combined Model for Analyzing the Interdependency of Electrical and Gas System. Proceedings of 2007 39th North American Power Symposium NAPS '07 2007; 468-472.

[15] Liu C, Shahidehpour M, Fu Y, Li Z. Security-Constrained Unit Commitment with Natural Gas Transmission Constraints. IEEE Transactions on Power Systems 2009; 24(3): 1523 – 1536.

[16] Wolf D, Smeers Y. The gas transmission problem solved by an extension of the simplex algorithm. Management Science 2000; 46(11): 1454-1465.

[17] O’Neill RP, Williard M, Wilkins B, Pike R. A Mathematical Programming model for Allocation of Natural Gas. Operation Research 1979; 27(5): 857-875.

[18] Ouyang L, Aziz K. Steady-state gas flow in pipes. Journal of Petroleum Science and Engineering 1996; 14(3-4): 137-158.

[19] Fu Y, Shahidehpour M, Li Z. Security-constrained unit commitment with AC constraints. IEEE Transactions on Power Systems 2005; 20(2): 1001-1013.

[20] Berard GP, Eliason BG. An improved Gas Transmission System Simulator. Society of Petroleum Engineers Journal 1978; 18(6): 389-398.

[21] Stoner MA. Sensitivity Analysis Applied to A Steady-state Model of Natural Gas Transmission System. Society of Petroleum Engineers Journal 1972; 12(2): 115-125.

[22] Li T, Eremia M, Shahidehpour M. Interdependency of Natural Gas Network and Power System Security. IEEE Transactions on Power Systems 2008; 23(4): 187-1824.
[23] Geoffrion AM. Generalized Benders decomposition. Journal of Optimization Theory and Applications 1972; 10(4): 237–261.
[24] Ma H, Shahidehpour M, Marwali MKC. Transmission constrained unit commitment based on Benders decomposition. Proceedings of 1997 American Control Conference 1997; 4: 2263-2267.
[25] Tomasgard A, Rømo F, Fodstad M, Midthun K. Optimization models for the natural gas value chain. In: Hasle G, Lie K-A, Quak E, editors. Geometric Modeling, Numerical Simulation, and Optimization: Applied Mathematics at SINTEF, New York: Springer-Verlag Berlin Heidelberg; 2007, p. 521-558.
[26] Roh JH, Shahidehpour M, Yong Fu. Market-Based Coordination of Transmission and Generation Capacity Planning. IEEE Transactions on Power Systems 2007; 22(4): 1406-1419.
[27] Roh JH, Shahidehpour M, Wu L. Market-based Generation and Transmission Planning with Uncertainties. IEEE Transactions on Power Systems 2009; 24(3): 1587-1598.
[28] Dupačová J, Gröwe-Kuska N, Römisch W. Scenario Reduction in Stochastic Programming: An approach Using Probability Metrics. Mathematical Programming 2003, A 95: 493-511.
[29] GAMS/SCENRED Documentation. Available from www.gams.com/docs/document.htm.

FIGURE CAPTIONS

TABLE CAPTIONS

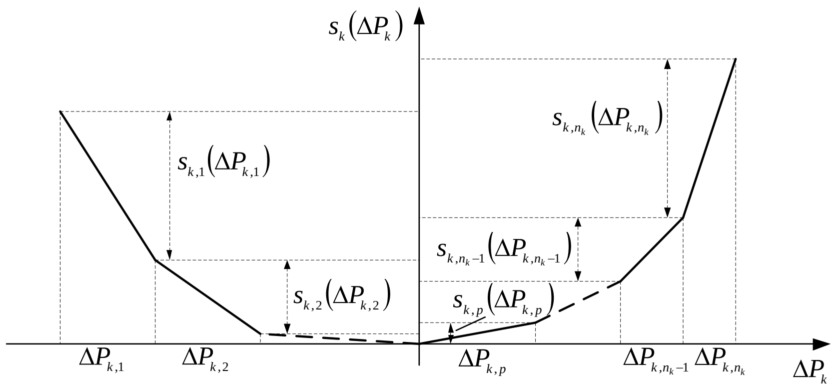

Figure 1: The bidding curve for MBCM of participant *k*

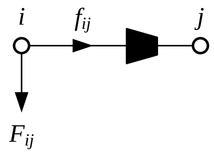

Figure 2: Modeling of compressor *i-j*

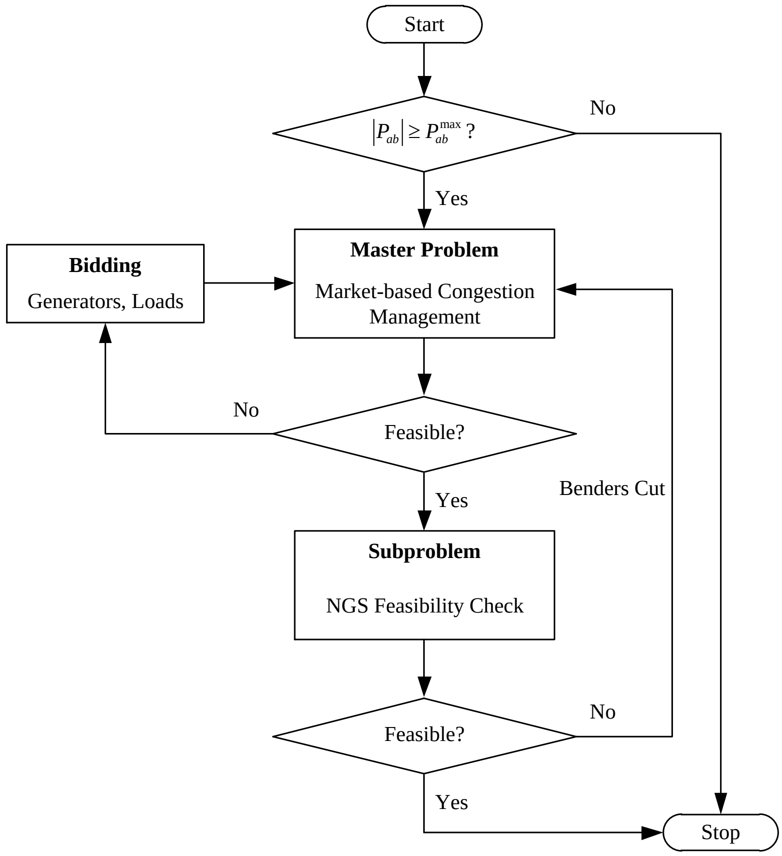

Figure 3: Flowchart of MBCM with NGS constraints

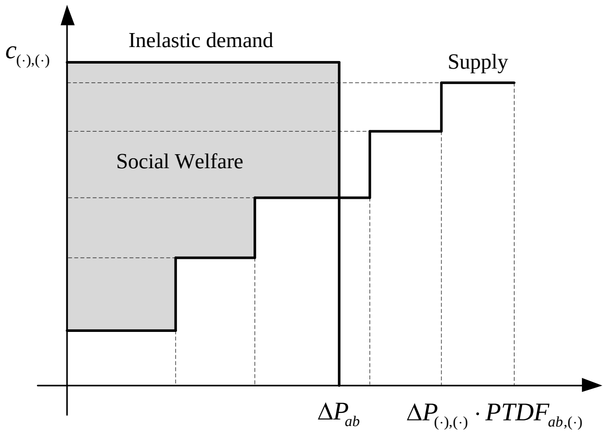

Figure 4: Demand and supply curves for MBCM on path a–b

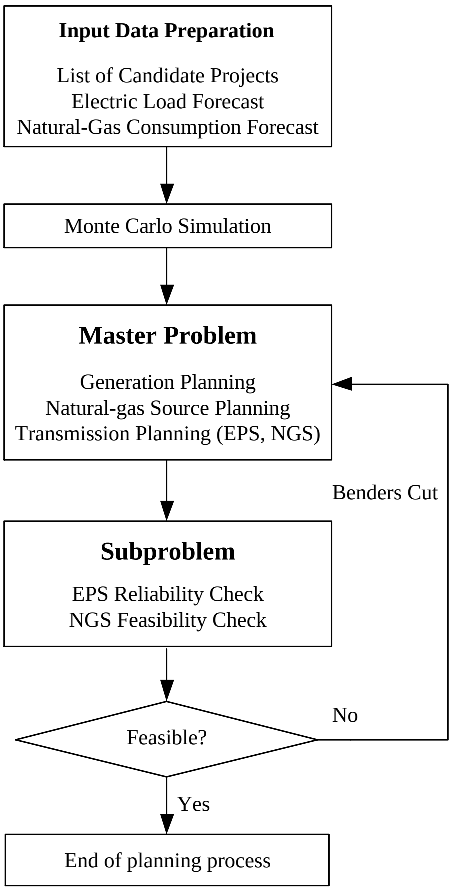

Figure 5: Coordinated long-term planning of EPS and NGS

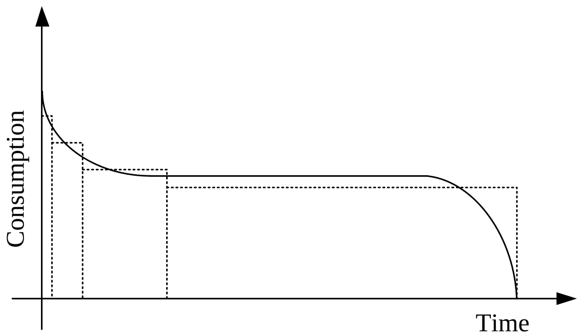

Figure 6: Annual load duration curve.

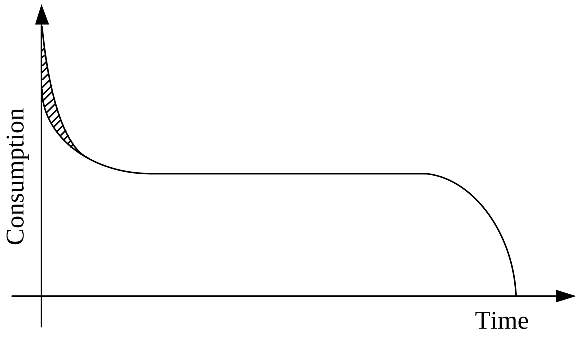

Figure 7: Modified annual load duration curve.

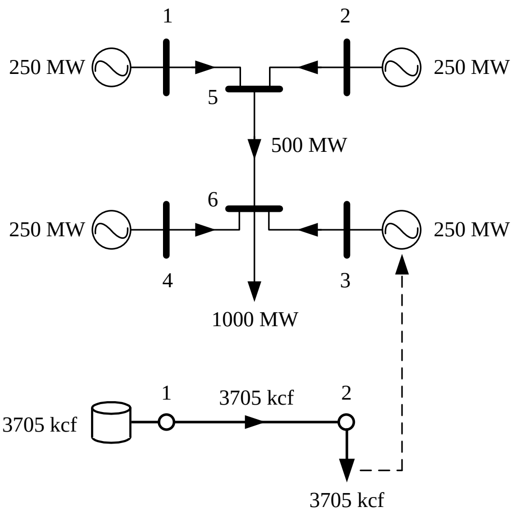

Figure 8: Six-bus EPS and two-node NGS

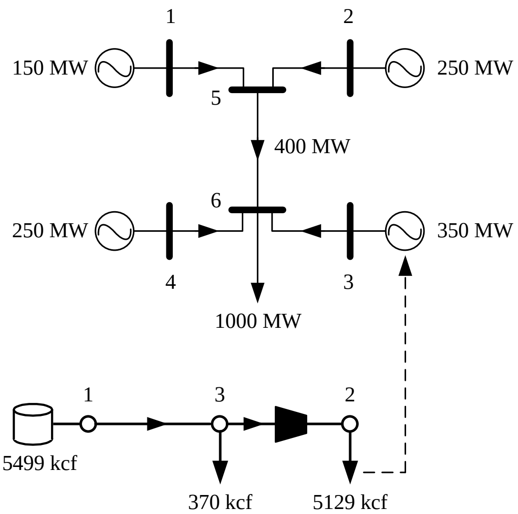

Figure 9: Six-bus EPS and three-bus NGS in case E

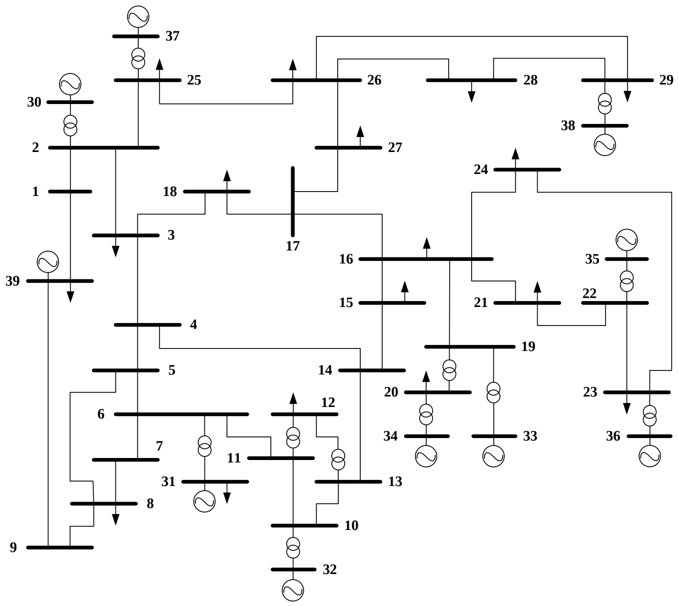

Figure 10: IEEE 39-bus model of EPS

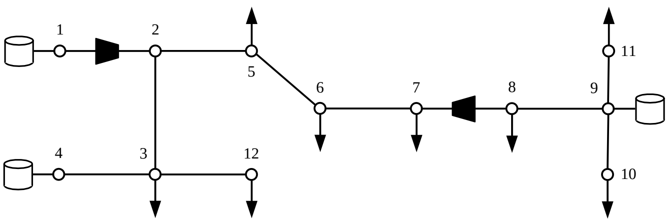

Figure 11: 12-node model of NGS

Table 1: Parameters of natural gas compressor in case E

Node i	Node j	α_{ij}	a_{ij}	b_{ij}	k_{ij} (kcf)	d_{ij} (kcf/MW)	e_{ij} (kcf/MW^2)
3	2	0.3	0.1	0.2	20	0.5	0

Table 2: Parameters of natural gas compressor in case E

Node i	Node j	H_{ij}^{min} (MW)	H_{ij}^{max} (MW)	R_{ij}^{min}	R_{ij}^{max}
3	2	700	800	1	2

Table 3: Results for six-bus EPS and two-node NGS for cases A–E

	A	B	C	D	E
P_1 (MW)	250	150	150	250	150
P_2 (MW)	250	250	250	250	250
P_3 (MW)	250	350	270.76	305.9	350
P_4 (MW)	250	250	329.24	294.1	250
$P_{5\text{-}6}$ (MW)	500	400	400	400	400
v_1 (kcf)	3705	5129	4000	4500	5499
l_2 (kcf)	3705	5129	4000	4500	5129
f_{12} (kcf)	3705	5129	4000	4500	5499
π_1 (Pig)	150	150	150	150	150
π_2 (Pig)	130.42	109.44	126.89	120	178.3
π_3 (Pig)	-	-	-	-	102
CM cost ($)	0	2500	3688.6	3161.5	2500

Table 4: Bids of generators in IEEE 39-bus EPS

Gen.	$\Delta P_{k,p}$ (MW)	$c_{k,p}$ ($/MW)
30	-50	-1
30	100	50
30	200	40
31	-100	20
31	300	40
32	-200	10
33	400	35
34	-20	10
34	300	20
35	100	35
36	-70	11
36	50	35
36	150	30
37	-40	50
37	30	25
38	-100	15
38	100	20

Table 5: Results for IEEE 39-bus EPS and 12-node NGS

	A	B	C
ΔP_{30} (MW)	0	0	48.14
ΔP_{31} (MW)	0	-100	-100
ΔP_{32} (MW)	0	-18.01	-15.92
ΔP_{33} (MW)	0	0	0
ΔP_{34} (MW)	0	3.33	-12.64
ΔP_{35} (MW)	0	0	0
ΔP_{36} (MW)	0	0	10.17
ΔP_{37} (MW)	0	14.67	0.15
ΔP_{38} (MW)	0	100	70.1
$S_{5\text{-}6}$ (MVA)	460.67	399.83	399.67
$Q_{5\text{-}6,0}$ (MVAr)	35.48	35.48	35.48
$Q_{5\text{-}6}$ (MVAr)	35.48	30.19	30.18
$S_{16\text{-}17}$ (MVAr)	223.39	189.45	187.69
$Q_{16\text{-}17,0}$ (MVAr)	12.23	12.23	12.23
$Q_{16\text{-}17}$ (MVAr)	12.23	8.99	8.83
CM cost ($)	0	4613.7	5922

Table A.1: Active and reactive power injections and generator limits of IEEE 39-bus system

Node k	Type	P_k (MW)	Q_k (MVAr)	P_k^{min} (MW)	P_k^{max} (MW)
1	PQ	0	0	-	-
2	PQ	0	0	-	-
3	PQ	-322	2.4	-	-
4	PQ	-500	184	-	-
5	PQ	0	0	-	-
6	PQ	0	0	-	-
7	PQ	-233.8	84	-	-
8	PQ	-522	176.6	-	-
9	PQ	0	0	-	-
10	PQ	0	0	-	-
11	PQ	0	0	-	-
12	PQ	-8.5	88	-	-
13	PQ	0	0	-	-
14	PQ	0	0	-	-
15	PQ	-320	153	-	-
16	PQ	-329.4	32.3	-	-
17	PQ	0	0	-	-
18	PQ	-158	30	-	-
19	PQ	0	0	-	-
20	PQ	-680	103	-	-
21	PQ	-274	115	-	-
22	PQ	0	0	-	-
23	PQ	-247.5	84	-	-
24	PQ	-308.6	-92.2	-	-
25	PQ	-224	47.2	-	-
26	PQ	-139	17	-	-
27	PQ	-281	75.5	-	-
28	PQ	-206	27.6	-	-
29	PQ	-283.5	26.9	-	-
30	PV	250	-	0	350
31	PV	521.3	-	0	750
32	PV	650	-	0	750
33	PV	632	-	0	732
34	PV	508	-	0	608
35	PV	650	-	0	750
36	PV	560	-	0	660
37	PV	540	-	0	640
38	PV	830	-	0	930
39	PV	-104	-	0	1100

Table A.2: Line and transformer parameters of IEEE 39-bus system

Bus i	Bus j	Type	R	X	B	Tap
1	2	Line	0.0035	0.0411	0.6987	0
1	39	Line	0.001	0.025	0.75	0
2	3	Line	0.0013	0.0151	0.2572	0
2	25	Line	0.007	0.0086	0.146	0
3	4	Line	0.0013	0.0213	0.2214	0
3	18	Line	0.0011	0.0133	0.2138	0
4	5	Line	0.0008	0.0128	0.1342	0
4	14	Line	0.0008	0.0129	0.1382	0
5	6	Line	0.0002	0.0026	0.0434	0
5	8	Line	0.0008	0.0112	0.1476	0
6	7	Line	0.0006	0.0092	0.113	0
6	11	Line	0.0007	0.0082	0.1389	0
7	8	Line	0.0004	0.0046	0.078	0
8	9	Line	0.0023	0.0363	0.3804	0
9	39	Line	0.001	0.025	1.2	0
10	11	Line	0.0004	0.0043	0.0729	0
10	13	Line	0.0004	0.0043	0.0729	0
13	14	Line	0.0009	0.0101	0.1723	0
14	15	Line	0.0018	0.0217	0.366	0
15	16	Line	0.0009	0.0094	0.171	0
16	17	Line	0.0007	0.0089	0.1342	0
16	19	Line	0.0016	0.0195	0.304	0
16	21	Line	0.0008	0.0135	0.2548	0
16	24	Line	0.0003	0.0059	0.068	0
17	18	Line	0.0007	0.0082	0.1319	0
17	27	Line	0.0013	0.0173	0.3216	0
21	22	Line	0.0008	0.014	0.2565	0
22	23	Line	0.0006	0.0096	0.1846	0
23	24	Line	0.0022	0.035	0.361	0
25	26	Line	0.0032	0.0323	0.513	0
26	27	Line	0.0014	0.0147	0.2396	0
26	28	Line	0.0043	0.0474	0.7802	0
26	29	Line	0.0057	0.0625	1.029	0
28	29	Line	0.0014	0.0151	0.249	0
12	11	Tr.	0.0016	0.0435	0	1.006
12	13	Tr.	0.0016	0.0435	0	1.006
6	31	Tr.	0	0.025	0	1.07
10	32	Tr.	0	0.02	0	1.07
19	33	Tr.	0.0007	0.0142	0	1.07
20	34	Tr.	0.0009	0.018	0	1.009
22	35	Tr.	0	0.0143	0	1.025
23	36	Tr.	0.0005	0.0272	0	1
25	37	Tr.	0.0006	0.0232	0	1.025
2	30	Tr.	0	0.0181	0	1.025
29	38	Tr.	0.0008	0.0156	0	1.025
19	20	Tr.	0.0007	0.0138	0	1.06

Table A.3: Parameters of natural-gas compressors of 12-node NGS

Node i	Node j	α_{ij}	a_{ij}	b_{ij}	k_{ij} (kcf)	d_{ij} (kcf/MW)	e_{ij} (kcf/MW^2)
8	7	0.15	0.1	0.17	25	0.028	0.0001
1	2	0.22	0.1	0.165	30	0.023	0.0001

Table A.4: Parameters of natural-gas compressors of 12-node NGS

Node i	Node j	H_{ij}^{min} (MW)	H_{ij}^{max} (MW)	R_{ij}^{min}	R_{ij}^{max}
8	7	300	400	1	2
1	2	150	330	1	2

Table A.5: Natural gas injections and well limits of 12-node NGS

Node i	v_i (kcf)	L_i (kcf)	v_i^{min} (kcf)	v_i^{max} (kcf)
1	2000	0	500	2000
2	0	0	-	-
3	0	-1000	-	-
4	3000	0	500	6000
5	0	-1500	-	-
6	0	-1500	-	-
7	0	-1500	-	-
8	0	-1500	-	-
9	8500	0	1000	15000
10	0	-1500	-	-
11	0	-2000	-	-
12	0	-3000	-	-

Table A.6: Type of nodes and pressure limits of 12-node NGS

Node i	Type	π_i^{min} (Pig)	π_i^{max} (Pig)
1	Load	120	150
2	Load	250	300
3	Load	220	250
4	Well	360	400
5	Generator 37	220	250
6	Load	230	250
7	Load	250	320
8	Load	130	180
9	Well	180	220
10	Load	130	200
11	Generator 38	130	200
12	Generator 34	150	220

Table A.7: Parameters of natural gas pipelines of 12-node NGS

Node i	Node j	c_{ij} (kcf/Psig)
2	3	16
2	5	8
3	4	10
3	12	25
5	6	5.3
6	7	20
8	9	45
9	10	20
9	11	13.5

Table A.8: Gas consumption coefficients of gas-fired units in IEEE 39-bus system

Bus i in EPS	Node j in NGS	p_i (kcf)	q_i (kcf/MW)	r_i (kcf/MW^2)
34	12	350	0.01	0.0118
37	5	25	0.03	0.005
38	11	1	1.6	0.001